Tuple Space Explosion: A Denial-of-Service Attack Against a Software Packet Classifier

Levente Csikor[†], Dinil Mon Divakaran[✳], Min Suk Kang[†], Attila Kőrösi[‡], Balázs Sonkoly[┼‡], Dávid Haja[‡], Dimitrios P. Pezaros[*], Stefan Schmid[ϒ], Gábor Rétvári[‡]
[†]National University of Singapore, [✳]Trustwave, [‡]Budapest University of Technology and Economics, [┼]MTA-BME Network Softwarization Research Group, [*]University of Glasgow, [ϒ]Faculty of Computer Science, University of Vienna

ABSTRACT

Packet classification is one of the fundamental building blocks of various security primitives and thus it needs to be highly efficient and available. In this paper, we evaluate whether the de facto packet classification algorithm (i.e., Tuple Space Search scheme, TSS) used in many popular software networking stacks, e.g., Open vSwitch, VPP, HyperSwitch, is robust against low-rate denial-of-service (DoS) attacks. We present the *Tuple Space Explosion* (TSE) attack that exploits the fundamental space/time complexity of the TSS algorithm. We demonstrate that the TSE attack can degrade the switch performance to as low as 12% of its full capacity with a very low packet rate (i.e., 0.7 Mbps) when the target packet classification only has simple policies, e.g., "allow a few flows but drop all others". Then, we show that if the adversary has partial knowledge of the installed classification policies, she can virtually bring down the packet classifier with the same low attack rate. The TSE attack, in general, does not generate any specific attack traffic patterns but some attack packets with *randomly* chosen IP headers and arbitrary message contents. This makes it particularly hard to build a signature of our attack traffic for detection. Since the TSE attack exploits the fundamental complexity characteristics of the TSS algorithm, unfortunately, there seems to be no complete mitigation of the problem. We thus suggest, as a long-term solution, to use other packet classification algorithms (e.g., hierarchical tries, HaRP, Hypercuts) that are not vulnerable to the TSE attack. As a short-term solution, we propose `MFCGuard`, a monitoring system that carefully manages the entries in the tuple space to keep packet classification fast for the packets that are eventually accepted by the system.

CCS CONCEPTS

• **Security and privacy → Denial-of-service attacks**.

1 INTRODUCTION

Packet classification is one of the fundamental building blocks of various security primitives. From access control implementation to network traffic isolation to denial-of-service defenses, they all require to classify incoming packets into multiple groups for different purposes, e.g., block/redirect certain traffic. Packet classification, thus, should be highly efficient, dependable, and available.

With the proliferation of virtualization techniques, packet classification has become softwarized and been widely used in virtualized systems today. As an example, Open vSwitch (OVS) [57] (along with many other software switches; e.g., VPP [26], HyperSwitch [59], GSwitch [76]) is universally used in virtualized environments. OVS is massively used for basic switching and firewall implementation for the tenants in cloud hosting systems enabling them to further specify custom firewall rules for their own purposes [15, 70] (§2). Moreover, dynamic filter rule updates for denial-of-service defense can be implemented with the software-defined networking (SDN) capability [8], particularly OpenFlow, in OVS [45].

In this paper, we evaluate whether the de facto packet classification algorithm widely used in many popular software switches (OVS as our running example) is robust against denial-of-service (DoS) attacks (§3). Our study has great importance since the targeted packet classification algorithm, namely, Tuple Space Search scheme (TSS) [64], is extensively used not only in traditional appliances but also in wide range of virtualized networked systems; just to name a few, software based intrusion detection systems [43], stateful NAT implementation [33, 48], cloud management systems [25, 71].

Our findings are alarming. Not only effective DoS attacks against the TSS packet classification are possible but also detection and mitigation of the attacks are hard. First, we present a new low-rate DoS attack, which we call the *Tuple Space Explosion* (TSE) attack (§3), against the TSS scheme (§4). We demonstrate that as little as 670 kbps of attack traffic from a single traffic source can easily degrade a single OVS instance from its full capacity of 10 Gbps to 2 Mbps when an adversary has a partial control over (or knowledge of) the access control rules installed in the targeted OVS (§5).When an adversary has no such access to her target (§6), we show, she can still achieve a significant degradation of 88% from the maximum capacity with low attack traffic volume.

One interesting aspect of the TSE attack is that it does *not* demonstrate any specific patterns of its attack traffic. Unlike the existing low-rate DoS attacks (e.g., algorithmic-complexity DoS attacks [16, 61], shrew attacks [42]) that send carefully-crafted attack packet sequences with specific traffic patterns to the target system, the TSE attack only requires *arbitrary* packet header fields and message contents, along with arbitrary packet arrival times. This makes its identification hard as it is not straightforward to define a specific signature of the attack traffic.

In fact that the TSE attack is highly effective only with randomly-generated inputs implies that the attack does not depend on specific attack strategies. Instead, it relies on the internal state of the target switch. That is, there exist certain states of the target switch that makes it vulnerable to DoS attacks with randomly-generated inputs. We investigate such system states in terms of Access Control Lists (ACLs) of the TSS packet classification. Unfortunately, some commonly used ACL patterns (e.g., `WhiteList+DefaultDeny`) are shown to be particularly vulnerable to the TSE attack.

Lastly, the very fact that the target of the TSE attack is the packet classifier itself makes it hard to design countermeasures. Defending against the TSE attack would require to have another packet classifier to filter out suspicious packets. However, unfortunately, the additional packet classifier is also likely vulnerable to the same DoS attack if implemented with the TSS algorithm. To mitigate the TSE DoS attack, thus, one has to deploy a different packet classifier that is robust against the TSE attacks. Yet, this suggests that this second packet classifier could have been simply used as the main classifier in the first place!

The TSE attack exploits the fundamental space/time complexity of the TSS algorithm and thus no complete mitigation of the problem seems possible (§7). Therefore, as a long-term solution, we suggest to use other packet classification algorithms that are not vulnerable to the TSE attack. Hierarchical tries [31], HaRP [58], and Hypercuts [10] packet classification algorithms seem to be unaffected by the TSE attack directly, although more in-depth study may be required for comprehensive analysis.

As a short-term solution, we present a cache management scheme, which we call `MFCGuard`, that dynamically monitors the number of entries in the tuple space and *removes* less important ones to lower the performance overhead of the packet classification (§8). We show that `MFCGuard` can limit the performance degradation for the packets that are eventually allowed to the system. This guaranteed performance for the allowed packets is achieved, however, at the expense of much increased processing time for the packets to be denied by the ACL rules. We discuss some operational concerns of `MFCGuard`, particularly when used in cloud hosting systems, where the increased computation overhead of `MFCGuard` may affect the operation of the tenants' workloads in the system.

2 BACKGROUND

Here, we describe the operation and fundamental building blocks of the most typical virtual switches, particularly, Open vSwitch (OVS) [57], and present the packet classification, called Tuple Space Search (TSS), used in OVS. Readers familiar with the packet classification algorithms in software switches may continue from §3.

2.1 Switching Stacks for Virtualization

Enterprises increasingly offload business-critical workloads to the public cloud to benefit from low infrastructure costs, high availability, and flexible resource provisioning. Reliable and efficient service provisioning heavily depends on the ability to efficiently switch traffic between the tenants' workloads and the outside world.

In this paper, we use OVS as our running example, but the presented vulnerabilities might affect other TSS-based software switches (e.g., VPP [26], Hyperswitch [59], GSwitch [76]). OVS [57] is an open source, multilayer, production quality software switch that enables massive network automation through programmatic extensions [1]. It can be managed remotely through standardized control plane protocols [52, 56]. The OVS *flow table* describes the packet processing behavior to be implemented by the switching logic at a high level. Due to its flexibility, generality, and community support, OVS has been extensively used in cloud deployments [1].

The flow table of an OVS switch is an ordered set of *flows*, where each flow is a pair of (1) a *wildcard rule*, operating on specific protocol header fields (e.g., IP source address, ports) and designating packets that belong to the flow, and (2) an *action*, a set of packet processing primitives to be applied to packets matching the flow rule; e.g., "forward to port", or "drop".

Two flows in the flow table are said to *overlap* if there is a packet header that matches both. In this case, the matching flow that occurs first in the flow table takes precedence. For instance, in the sample ACL in Fig. 6, a packet with source IP address `10.0.0.1`, source and destination ports `34521`, and `443`, respectively, matches both the second and the last flow entries with the first flow overriding the last one by higher priority.

In contrast, a flow table in which all rules are disjoint is *order-independent* because all packets have a single matching rule and equal priority (i.e., order is irrelevant). In general, this makes packet classification much simpler [41].

Most software switches (if not all) support order-dependent flow tables despite the performance benefit of order-independent tables because of the flexibility of the former. In virtualized environments (e.g., multiple tenants share a single software switch for access control), users with various networking knowledge configure the flow rules in the switches. The greater flexibility of order-dependent tables support rule wildcarding and flow priorities, which allow complex packet processing logics to be described concisely.

2.2 TSS for Fast Packet Classification

To cut down the prohibitive cost of packet classification, OVS adopts the well-known fast path/slow path separation principle [50]. The fast path comprises two layers of *flow caches*, and the slow path implements a complete representation of the flow table serving as a fallback when the fast path cannot decide on the fate of a packet. Only the first packet of each flow is subjected to full-blown flow-table processing, i.e., slow path, and the resulting flow-specific rules and actions are then registered in the flow caches; the rest of the flow's packets take the fast path. This amortizes the cost of packet classification over subsequent packets of a flow, contributing to increased performance without loss of expressiveness and generality [13, 39, 46] (cf. §11.1 for the general flow-cache hierarchy).

Within the fast path, the *microflow cache* implements a per-transport-connection exact-match store where lookup occurs over *all* header fields, while the *megaflow cache* (MFC) bundles multiple microflows into a single megaflow to impose common processing to the entire bundle [29, 48, 63]. In this design, the microflow cache merely serves as "short-term" memory and it is often exhausted even in normal operation (by default, it contains only a couple of hundred entries). The lookup algorithm in the MFC relies on the TSS scheme [64], the prevailing packet classifier used to implement ACLs in other hypervisor switches as well (e.g., VPP [26], HyperSwitch [59], GSwitch [76]). MFC generally saves on cache entries by a single megaflow covering, say, all incoming HTTP connections regardless of the source TCP port (i.e., TCP port wildcarded). In a nutshell, this is done by collecting the entries matching on the same set of header bits into a hash in which masked packet headers can be found fast. Then, masks and associated hashes are searched sequentially until the first matching entry is found.

Note that the TSS implementation in OVS does not know about flow priorities; thus the slow path ensures that MFC entries are

all disjoint to make packet classification simpler yet introducing worst case exponential complexity (i.e., exhaustive linear search in the different masks). Correspondingly, as long as the number of masks is kept in a reasonable range (e.g., couple of hundreds masks), packet processing in the fast path is close to line rate. This property of the TSS is the very logic we aim to exploit in this paper.

3 TUPLE SPACE EXPLOSION: OVERVIEW

Here, we provide a high-level overview of the attack. First, we describe our threat model, then we show the essence of the proposed TSE attack and discuss the algorithmic complexity vulnerability of the TSS scheme using its implementation in OVS. Then, we show two different approaches of TSE, each posing different requirements and targets for the attacker.

3.1 Threat Model

We consider a general virtualized computing environment, where a targeted software switch is used for packet processing and basic network operations. This includes a typical multi-tenant cloud infrastructure whereby tenants lease resources in the cloud to deliver public services. Tenants may use cloud management system (CMS) APIs to set up their access-control list (ACL) rules in the underlying software switch to access-control, redirect, or log accesses to different resources [15, 35–37]. We consider that the internal algorithms of the data plane fabric is fully known to adversaries.

The attacker's goal is to send some attack packets to the virtual switch, which when subjected to the implemented ACL will exhaust the underlying resources denying access to the rest of the users.

The adversary only needs to have the capability of crafting and sending IP packets with arbitrary legitimate headers without being filtered at the first hand; e.g., by her upstream or transit ISPs.

Note that we do not require any privilege of the target switch for the effective DoS attack. However, having some partial, internal state of the target switch (e.g., installed ACL rules) can further improve the efficiency (i.e., less number of required attack packets).

Here, we do *not* consider volumetric DoS attacks that congest the target's network bandwidth with attack traffic.

3.2 DoS with Excessive MFC Masks

As mentioned in §2.2, the lesser the number of masks in the MFC the much faster the packet classification is.

To provide a simple but useful intuition oh how easily this number can be increased, consider that in a hypothetical protocol (say, *HYP*) having only 3 relevant header bits and consider a 3-bit-wide "Whitelist+DefaultDeny" type flow table shown in Fig. 1. The MFC is an unordered set of key-mask pairs $\mathcal{C} = \{(K, M)\}$ with entries $C = (K, M)$; here, M is a bitmap to mask relevant header bits and K is a key to be matched on the masked bits. According to the TSS scheme, we maintain a list of distinct masks $\mathcal{M}$ (the "tuple space") plus, for each mask $M \in \mathcal{M}$, a hash H_M that will be used to store and lookup the keys with mask M.

Suppose that the switch receives a packet with *HYP* header $h_1 = 001$. Since, initially, the MFC is empty, the packet is deferred to the slow path, which finds the first flow in the flow table to match, associates the action `allow`, and installs a new key-mask pair $C_1 = (001, 111)$ into the MFC; this amounts to adding the new mask 111 to the mask list $\mathcal{M}$ and storing the key 001 in the respective hash H_{111}.

Now assume that a second packet arrives with header $h_2 = 111$. In this case, MFC lookup occurs as follows: take each mask $M \in \mathcal{M}$ one by one, apply M to the header and look up the resulting bitvector in the corresponding hash H_M; if the lookup succeeds, then return a cache hit; otherwise resort to the next mask. In this case, there is only a single mask $M = 111$, so we look up the key $(h_2 \ AND \ M) = 111$ in H_{111}. Since the lookup fails, this is a cache miss. The slow path will find the `drop` rule to match, and it will insert a new MFC entry into the fast path.

At this point, there are multiple choices to generate a new entry, each striking a different balance between space- and time-complexity (see details in §4); which one is taken in any particular case is the result of a rather involved construction of heuristics in the OVS slow path [57]. In a nutshell, when generating a new MFC entry C for a packet with header h, OVS maintains the following two invariants:

Inv(1) *Cover:* h matches C.
Inv(2) *Independence:* C is disjoint from any $C' \in \mathcal{C}$.

Inv(1) simply states that an MFC entry will match the packet header that sparked its generation. Inv(2) greatly simplifies the fast path code because lookup can early-exit once the first match is found, instead of having to tediously search through the entire mask list to check whether higher-priority matches occur later in the list (cf. Alg. 1 in §11.2). Hence, $h_2 = 111$ can spawn a new key-mask pair of either $C_2 = (111, 111)$ or $C_2 = (111, 100)$, covering 1 or 4 packets, respectively, according to different strategies (cf §4.1).

One might realize that due to these invariants, the number of key-mask pairs covering all possible packets significantly increases with the number and bit-width of the headers the ACL matches on. Particularly, if we establish a logical `OR` relation between the `allow` rules on more header fields (see a typical example in Fig. 6), it will in turn create an `AND` connection on the `drop` rule. Therefore, in order to test each header field *at the same time*, we need to test each combination of key-mask pairs for the individual headers resulting in a *multiplicative increase in the tuple space* (cf. §4.2).

This means that a typical ACL matching on the IP source address and TCP ports (e.g., ACL in Fig 6) can easily result in thousands of MFC masks. Consequently, this type of security policies/ACLs with an `OR` relation between the targeted header fields can become the sweet-spot for our attack; *hence the name Tuple Space Explosion.*

Next, we briefly present two different approaches of the TSE attack based on the partial control an adversary can have over the ACL. Then, in §4, we give a comprehensive overview of the look up algorithm, analyze its space- and time-complexity as the number of headers grows, and go through each case step-by-step to show how the MFC is exactly being managed.

3.3 Two Approaches of the TSE Attack

Before, we have seen that in order to practically populate the MFC with new entries and masks, we need to send a specially crafted packet sequence corresponding to the installed ACL. For instance, sending packets with `(HYP)` header `{001}` and `{100}` towards to the ACL shown in Fig. 1 will spawn entries #1 and #2 in the MFC as depicted in Fig. 3. However, a subsequent packet with header

{101} will be also "caught by" entry #2, hence not increasing the number of masks in the MFC. Correspondingly, being aware of the ACL itself is a key aspect to the efficiency of the TSE attack. Thus, we present two different approaches of the TSE attack each posing different requirements and targets for the attacker.

In order to explain the main differences between them, and their practical targets, we need to understand a key abstraction in a cloud environment: the *per-user virtual switches* tenants configure to set up their ACLs. Tenants perceive these virtualised resources as their own physical switch, however switches are only logically separated and all of them are implemented and managed by the same individual software switch instance. Therefore, all workloads happened to be scheduled to the same hypervisor inherently share the switching fabric as well (e.g., the MFC).

Co-located TSE. We build on top of this abstraction: the attacker has leased resources in the cloud, which inherently makes him/her capable of installing ACLs into its own virtual switch. Then, the shared MFC can be easily populated with new masks by targeting the known ACLs (see details in §5). However, co-location comes at a price that only those tenants' workloads are affected that happened to be scheduled to the same hypervisor.

General TSE. In this approach, we alleviate the restrictions of *Co-located TSE*: we consider the case when the attacker has neither resources in the cloud, nor knowledge about any ACLs. Here, we investigate how much more effort an attacker needs in order to achieve the same efficiency as *Co-located TSE* (see later in §6).

4 SPACE – TIME COMPLEXITY OF TSS

Next, we analyze the space- and time-complexity trade-offs of the TSS scheme using its implementation in OVS as a typical example. Then, we show how the TSS scheme manages its data structure, and how to maximize the number of masks in the MFC step-by-step.

Clearly, the most time-consuming step in Alg. 1 is the iteration through the mask list $\mathcal{M}$, assuming that a hash lookup in H_M is $O(1)$; the more the masks the slower the algorithm. The space-complexity is in turn driven by the sheer storage size of the MFC entries. Our observations are as follows.

Observation 1. *The time-complexity of TSS lookup grows linearly with the number of distinct masks as $O(|\mathcal{M}|)$ and the space-complexity grows linearly with the number of entries as $O(|C|)$.*

Next, we demonstrate that the complexity of cache lookup can become prohibitive due to an algorithmic complexity vulnerability in the underlying TSS scheme. In particular, we show specific corner cases for which the MFC will exhibit exponential space- and/or time-complexity. For simplicity, we carry on with the hypothetical 3-bit protocol example (cf. Table 1), but bear in mind that MFC works the same for arbitrary wide bit-widths of header fields.

4.1 Maximize MFC Masks: Single Header

Packet classification is conceptually easier when there is only a single packet header field, e.g., IP protocol or destination address in the flow rules [30, 63]. First, we concentrate on this case, i.e., when the network policies match on a single header field only. Consider again the simplified policy on 3 bits mentioned in §3.2, i.e., when packets with header *HYP* 001 is allowed and everything else is denied. Next, we discuss some possible strategies to construct the MFC for this ACL using TSS.

Wildcard rule	Action
0 0 1	allow
* * *	deny

Figure 1: Sample flow table

#	Key	Mask	Action
#1	000	111	deny
#2	001	111	allow
#3	010	111	deny
...	...	...	deny
#8	111	111	deny

Figure 2: Exact-match

#	Key	Mask	Action
#1	001	111	allow
#2	100	100	deny
#3	010	110	deny
#4	000	111	deny

Figure 3: Wildcarding

An invalid strategy would be to install the flow table as is into the MFC resulting in two masks and two MFC entries. However, this would *violate the independence invariant* as the two entries overlap: a packet with *HYP* 001 would match both MFC entries, which would confuse the lookup algorithm. Consequently, in order to load a flow table into the MFC, it first needs to be converted into an order-independent form.

Exact-match strategy. One trivial order-independent transformation would be to cover the entire range of *HYP* with a single completely filled exact-matching hash, resulting in the TSS setup depicted in Fig. 2. Since we have a single mask, TSS lookup is extremely fast (cf. Observation 1). However, we need to add all possible 8 keys that can occur on 3 bits to the hash, yielding a larger memory footprint. Note that in general, the exact-match technique yields optimal time-complexity with exponential space-complexity.

Wildcarding strategy. The opposite extreme would be to wildcard as many bits as possible in order to get the broadest possible rules, and the fewest hashes, in TSS. Here, we obtain an exact-match entry for the allow-rule and separate key-mask pairs for testing each of the related 3 header bits to cover the whole tuple space. First, check whether the most significant bit is set and, if it is, then drop the packet; then, test for the second bit provided that the first bit is not set, and so on. One can easily check in Fig. 3 that the resulting MFC is order-independent and it is the smallest possible representation of this kind. We obtain 4 entries and 3 masks (the first and the last entries have the same mask), reducing the space complexity from 8 megaflows to just 4 at the cost of increasing classification time from a single iteration of the TSS lookup algorithm (Algorithm 1) to possibly 3 iterations for the 3 masks. Apparently, each strategy gives a different compromise between space- and time-complexity (in line with [27, 32]). The below theorem characterizes the attainable tradeoffs in general TSS (see proof in the Appendix).

Theorem 4.1. *Given an ACL on a w-bit header field comprising a single exact-match* allow *rule and a lower-priority DefaultDeny policy, no TSS construction can achieve better than $O(k)$ time with $O(k2^{\frac{w}{k}})$ space complexity, for $1 \leq k \leq w$.*

Here, the parameter k balances between time- and space-complexity: for $k = 1$, we get optimal time-complexity ($O(1)$ time with $O(2^w)$ space), for $k = w$ we get optimal space-complexity ($O(w)$ time with $O(w)$ space), and different settings for $1 \leq k \leq w$ give different tradeoffs. While the compromise a particular TSS implementation realizes in a setup depends on a lot of unknowns,

HYP	HYP2	action
001	*	allow
*	1111	allow
*	*	deny

Figure 4: ACL on 2 headers

#	HYP	HYP2	Action
#1	001	****	allow
#2	1**	1111	allow
#3	01*	1111	allow
#4	000	1111	allow
#5	1**	0***	deny
#6	01*	0***	deny
#7	000	0***	deny
...	...	...	deny
#14	1**	1110	deny
#15	01*	1110	deny
#16	000	1110	deny

Figure 5: Corresponding MFC (keys are masked)

in practice OVS usually leans toward the "wildcarding" strategy (k close to w), striving to minimize the memory footprint of the fast path classifier even at the cost of crippling lookup efficiency (see the comments in `classifier.h` in the OVS source code).

In essence, this means that for *a single header of bit-width w, the MFC will have w masks* (in the worst case). However, in certain cases, OVS seems to optimize for the other extreme and minimizes lookup time at the cost of exponential space (k close to 1); we have seen such behavior for ACLs including IPv6 address fields (cf. §5.4).

4.2 Maximize MFC Masks: Multi Headers

Next, we generalize the single-field technique to multiple fields to get the desired exponential complexity in *any* TSS implementation.

As mentioned before, an ACL that filters on the 32-bit IPv4 source address field ($w_1 = 32$), we can generate 32 masks and 33 entries. For the port field ($w_2 = 16$), the corresponding figures are 16 masks and 17 entries, respectively. Establishing a logical `OR` relation, on the other hand, between different header fields in the ACL at the same time will in turn create an `AND` connection on the `drop` rule. Considering our example ACL in Fig. 4, this means that a packet can be dropped only if *both HYP* is not `001` *and HYP2* is not `1111`. We can see that the most space-efficient way to test the `deny` case individually for the *HYP* field is to test each bit one by one and similarly for *HYP2* field. However, collectively testing the two fields involves testing each combination of bit positions in the two fields (cf. Fig. 5), yielding $3 * 4 + 1 = 13$ masks with roughly the same number of entries[1]. Observe that the first allow rule of the ACL is represented in the MFC in the same way, which does not apply for the second allow rule (hence +1 in the above equation).

Theorem 4.2. *Given an ACL on n header fields of bit-width w_1, w_2, ..., w_n, comprising n `allow`-rules, each exact-matching on a single header field, plus a lower-priority DefaultDeny policy, no TSS construction can achieve better than*

$$O\left(\prod_i k_i\right) \quad \textit{time-complexity and}$$

$$O\left(\prod_i k_i \left(2^{\frac{w_i}{k_i}} - 1\right)\right) \quad \textit{space-complexity}$$

for any $1 \le k_i \le w_i$, $i \in \{1, \ldots, n\}$.

[1]Note that if the second rule (in Fig. 4) also filtered on *HYP*, we would still have roughly the same masks; only allowance would change.

Here, again the formula allows to tune the space–time tradeoff, but this time separately for each field through setting $1 \le k_i \le w_i$. For the extreme choice $k_i = 1$ for all i, we again get optimal time ($O(1)$ time with $O(2^{\sum_i w_i})$ space) and $k_i = w_i$ yields optimal space ($O(\prod_i w_i)$ for both time and space), and different settings for k_i again provide different tradeoffs. In practice, we observed again OVS to lean towards space minimization yielding the required multiplicatively scaling $O(\prod_i w_i)$ space- and time-complexity.

5 CO-LOCATED TSE

In this section, we discuss the *Co-located TSE* attack in detail. First we show the basic idea behind generating an "adversarial" packet sequence corresponding to the installed ACL. Then, we present a typical ACL tenants usually deploy for their services, and we apply our technique to show the efficiency of *Co-located TSE*. In particular, we evaluate *Co-located TSE* in various synthetic and live testbeds, and we show to what extent the tuple space explosion phenomenon can degrade the overall performance with considering several hardware offloading techniques.

5.1 Adversarial Packet Trace

As discussed in §3, to practically spawn the MFC entries, we need a specially crafted packet sequence. Note that such packets are completely legitimate and benign just as the useful user traffic. Taking the example ACLs in §4.1 and §4.2, first we consider only a single header, then we turn to the case of multiple headers.

Single Header. We found the following packet trace generation strategy against the *single header* scenario to work well in practice: generate a packet that matches the `allow` rule, then add a packet with each of the relevant bits inverted one-by-one. In Fig. 1, this results in the following *HYP* header fields: {`001, 101, 011, 000`}. It can be seen that packets with these headers will exactly result in the 4 MFC entries and 3 masks shown in Fig. 3.

Multiple Headers. We generalize from the single-field case to the multi-field case with minimal modification. Consider the extended sample ACL in Fig. 4. First, create the *HYP* list L_{HYP} according to the bit-inversion method, then create a similar list L_{HYP2} for the *HYP2* field, and then generate a packet with setting *HYP* and *HYP2* from the outer product of the lists $L_{\mathsf{HYP}} \times L_{\mathsf{HYP2}}$. Ignoring the packets for the second `allow` rule that do not generate new masks (see entries #2 – #4 and #14 – #16 in Fig. 5), this technique gives exactly $4 * 3 + 1 = 13$ packets and the same number of MFC masks. We omit the formal proofs here for brevity.

5.2 Practical ACLs

The effectiveness of the attack depends on the number of MFC masks the attacker can spawn in the data plane, which in turn depends on the number, bit-width and the values of the header fields the installed network policies match on. Correspondingly, as a full-blown attack we can target 3 IP header fields out of the possible IP 5-tuple: the source IP address, the source transport port, and the destination port[2] (see Fig. 6). Accordingly, we distinguish between several use cases, each with its own set of targeted header fields and its own expected effectiveness (the numbers are for IPv4).

[2]Non-IP packets not destined to the service will never reach the hypervisor.

Rule id	ip_src	tcp_src	tcp_dst	action
#1	*	*	80	allow
#2	10.0.0.1	*	*	allow
#3	*	12345	*	allow
#4	*	*	*	deny

Figure 6: Simple ACL of a full-blown TSE attack.

Table 1: HW/SW and orchestrator versions.

Property	Synthetic	OpenStack	Kubernetes
CPU	Intel Xeon E5-2620 v3		2 x Intel i5-6300U
Memory	64GB		2 x 2GB
NIC	Intel X710	Intel 82598	virtio
SmartNIC	Mellanox CX-4	–	–
Kernel	4.13.13-1	4.4.0-112	4.4
OVS	2.9.2 (stable)	2.9.90 (unstable)	2.7
Orchestrator	–	OpenStack Queens	Kubernetes 1.7

First, in case of Baseline, there is only one allow rule (apart from the simple DefaultDeny rule) in the flow table, which allows the tenant's service to be reached (e.g., rule #1 in the ACL in Fig. 6). Accordingly, there is one benign traffic flow matching on that single rule only, and no malicious traffic enters the system; #MFC masks: 1. This scenario represents the full capacity of the switch in normal operation and serves as a baseline to measure service degradation for the rest of the use cases.

In case of Dp, we attack on a single header field, the 16-bit destination port. Accordingly, the ACL contains only Rule #1 and Rule #4 from the full-blown setup of Fig. 6, but now adversarial traffic against rule #1 is sent; #MFC masks: 16. Then, we gradually increase the number of headers and combine them, starting from the basic multi-field attacks of SpDp and SipDp, targeting both port (#MFC masks:$\sim 16^2 = 256$), and the IP source address with the destination port fields (#MFC masks: $\sim 32 * 16 = 512$), respectively.

Finally, as a full-blown attack, in SipSpDp we target all rules in Fig. 6 (#MFC masks: ~ 8200). Note that in all cases the traffic traces also include some additional random noise added to "unimportant" header fields (e.g., varying TTL) to increase the entropy hence using up the *microflow* cache.

5.3 Environments and Setup

Next, we present the setup used to evaluate *Co-located TSE* attack in various live environments. First, we present synthetic measurements on a standalone switch to show that the *TSS implementation in OVS is vulnerable to TSE attacks*. We also demonstrate that even *if the TSS implementation is offloaded to the hardware*, such a system is *still vulnerable*. Then, we study the performance of OVS when used as a hypervisor switch in a real OpenStack and a Kubernetes environment (small in-house testbeds for ethical reasons). Table 1 lists the software and hardware configurations used for the tests.

In these environments, we measure the raw throughput of a standalone OVS by simulating the pipeline that would arise in a real cloud deployment. We created a simplified cloud infrastructure consisting of a small data center (DC) having 2 servers hosting the tenants' workloads (see Fig. 7). In particular, the victim has a publicly available web service (V1 in Server 1), which s/he has installed an ACL (ACL-V) for. Furthermore, the victim also has another service (V2) used as a backend service of V1 scheduled to Server 2. On the other hand, the attacker also has a leased resource (A1) co-located with V1 in Server 1. Similarly, the attacker also defines

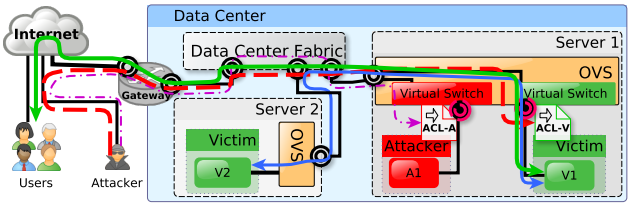

Figure 7: Simplified cloud infrastructure model and overview of *Co-located TSE* (thin dot-dashed purple line) and *General TSE* (thick red dashed line) attacks.

an ACL (ACL-A) for his/her own service (again, A1). However, in this case the attacker installs the ACL used for the full-blown TSE attack (cf. Fig. 6), and will send a corresponding packet sequence to it in order to populate the MFC with an excess amount of masks; hence potentially degrading the quality of services of other tenants' (i.e., V1 in this case). Furthermore, since the attainable number of masks is known, measurements do not require multiple runs.

5.4 Synthetic tests

Here, similarly to [59], our simplified DC consists of a system-under-test (SUT) which runs OVS acting as a hypervisor for two KVM virtual machines (Server 1), connected back-to-back to a similar "test" machine (Server 2). Instead of having a third machine for the incoming user traffic, for brevity, we only run an `iperf`[3] session between V1 and V2 (cf. Fig. 7). This represents the "useful" benign traffic (e.g., frontend – backend communication), whose performance degradation will demonstrate the collateral damage. Furthermore, the attacker, from which we generate the malicious traffic (via replaying a `pcap` file like in [19]), is also cast to Server 2 in a second VM[4]. The attack traffic, furthermore, contained the destination IP address of `A1`. (This setup gives a conservative estimate of the damage done; a single large "victim" flow can be handled in TSS using only a single cache entry "ideally", while real workloads usually include thousands of flows requiring hundreds of TSS entries that will compete with the attacker's adversarial cache entries.). The OVS flow table was bootstrapped manually according to the ACL in Fig. 6.

Next, we show to what extent the throughput of OVS is affected as the number of MFC masks increases; we also evaluate the effect of several NIC driver offloading techniques.

The results when the victim generates TCP and UDP traffic are depicted in Fig. 9a, where the x axis shows the number of MFC masks, while the y axis plots the corresponding throughput; note that both axes are in log scale. In order to easily realize the maximum number of MFC entries attainable in each use case, we note the x tick labels for numbers 17, 260, 516 and 8200 by Dp, SpDp, SipDp, and SipSpDp, respectively. We observed dramatically different effects depending on various settings of the NIC driver. In particular, *jumbo frames* and *generic transmit/receive offload* support (GRO ON) let the NIC to assemble many small TCP packets into a

[3]Even though benign traffic may consist of other types of flows (e.g., short-lived), they are out of scope of this study.
[4]Note, however, that in real deployments the attack might cannot be launched completely within a DC due to the IP spoofing protection mechanism of the CMS (e.g., OpenStack) that prevents attacks based on this header field.

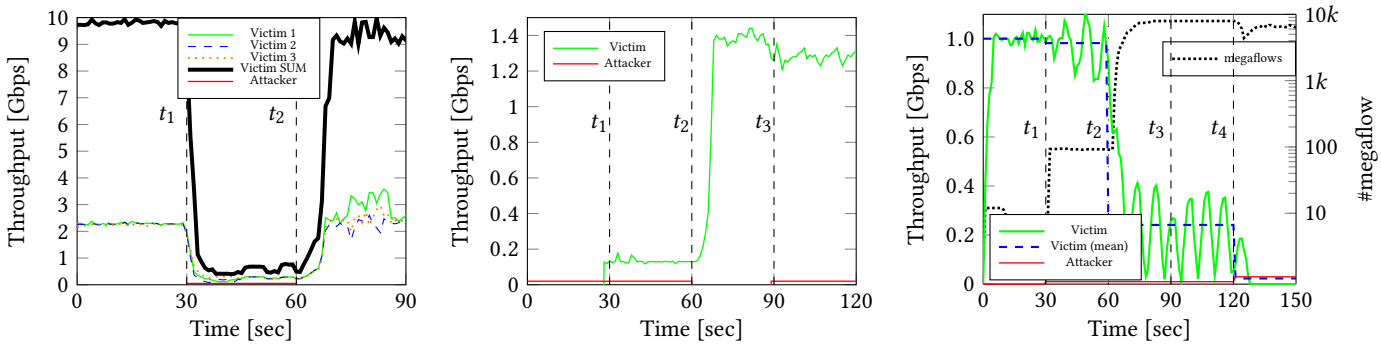

(a) Results for 3 concurrent TCP victim flows. (b) OpenStack results for the SipDp scenario. (c) Kubernetes results for the SipSpDp scenario.

Figure 8: Results for synthetic (a), OpenStack (b) and Kubernetes (c) scenarios, respectively

single large TCP buffer [59], reducing the effective traffic rate seen by OVS to a couple of thousand pps which it can process efficiently even when the TSS classifier has excess masks. Furthermore, we also enabled full hardware offloading (FHO ON) via our Mellanox CX-4 NIC, which gave a huge boost to the overall performance (~ 30 Gbps). However, the TSS classifier still remains vulnerable resulting in a significant performance drop as the number of MFC masks increases above 200. For UDP, these settings take no effect and performance degradation is clearly visible in all scenarios.

Our observations are as follows: *i)* 17 masks (max. in Dp use case) are sufficient to reduce the effective throughput to roughly 97%, 88%, and 53% of the Baseline with GRO ON, FHO ON, and GRO OFF, respectively. As the *ii)* number of masks reaches 260 (max. in SpDp), these numbers are as follows: 95%, 43%, and 10%, respectively. In case of having *iii)* more than 500 masks in the MFC (e.g., in SipDp), the increased packet classification time reduces the full capacity to its 76%, 29%, and 4.7%, respectively. Finally, *iv)* spawning more than 8000 masks (attainable in case of SipSpDp) result in virtually a complete denial of service attack in each case as the throughput drops down to 3.9%, 2.1%, and 0.2%, respectively. Hereafter, we present only the results for TCP with GRO OFF.

To present the increased packet processing time, the secondary y axis shows the flow completion time of 1GB TCP traffic with GRO OFF as the number of MFC masks grows; again, note the log scale. It can be seen that, on average, the flow completion time only increases half as high as the number of MFC masks.

Nevertheless, this experiment clearly marks the vulnerability of TSS to low-bandwidth DoS attacks.

Next, Fig. 8a gives the results for 3 parallel victim TCP flow in the SipDp scenario with TCP offloading disabled. In this benchmark, the attacker is active from t_1 until t_2 injecting 100 packets per second (50 Kbps), reducing victims' aggregate traffic rate from 9.7 Gbps to below 0.5 Gbps. Observe the delay in the recovery of the victim rate that returns to full rate only after 10 seconds after t_2; this is due to the 10 sec idle MFC timeout in OVS, keeping the attacker's entries alive for an extended time.

The extent and type of the damage varies on a case by case basis, depending on the type of ACLs injected, the OVS version, the NIC configuration, etc. For instance, when we apply the SipDp attack vector over IPv6 we find that OVS applies the "wildcarding" TSS entry generation technique only to the TCP destination port field but seems to handle the IPv6 source address using exact matching, which can result in only a handful of masks but hundreds of thousands of MFC entries (irrespectively of the TSE method). Hence, in this scenario the adversarial effect manifests itself not in the slowdown of the victim traffic but rather in excess memory and CPU consumption, with OVS taking up 8 CPU cores trying to uselessly reclaim megaflow memory occupied by the excess TSS entries. Restricting OVS to just 2 CPU cores then reduces victim traffic to 5% of its nominal rate.

Next, we evaluate the *Co-located TSE* attack in two smaller real testbeds (in-house for ethical concerns): OpenStack and Kubernetes.

5.5 OpenStack

Our OpenStack testbed (cf. Table 1 for details) uses the OVN integration [72]; this configuration is known to exhibit superior network performance compared to the default [4]. Workload isolation between the attacker and the victim was enforced by deploying the corresponding VMs using different OpenStack tenants.

The CMS API only allows the SipDp scenario, for which the results are given in Fig.8b; here, the attacker starts sending at the beginning of the benchmark at 100 pps and stops in the 60-th second only to restart 30 seconds later; the victim joins with a full-rate UDP `iperf` session at the 30-th second. In line with the synthetic setup, *in the OpenStack testbed we again see a substantial (more than 90%) useful performance reduction during the time interval when both the attacker and the victim are active.* Again, the victim recovers 10 seconds after the attacker stops sending. Curiously, the re-activation of the attacker causes only a minor damage to the victim rate (about 10% drop); it seems that the attack is effective only against newly established target flows but causes minor harm to long-lasting flows already active at the moment when the attack starts. We observed this behavior consistently in this version of OpenStack; we have contacted the OVS authors regarding this behavior of this specific unstable version of OVS, but the reasons were mostly unknown and migrating to a stable version was suggested.

5.6 Kubernetes

Our setup uses the OVN integration [68] and the topology is the same as in the synthetic tests; one server hosts the attacker and the victim source and another hosts the sinks, both provisioned in separate vagrant boxes connected by a *virtio* network link supporting 1

Gbps rate. Here, we could use the SipSpDp attack scenario yielding the full ACL in Fig. 6; since Kubernetes/OVN currently does not support the full semantics of Calico network policies we injected the source port filtering rules manually via the CLI.

The results are shown in Fig. 8c. Initially no "malicious" ACL is set up, i.e., when the victim starts an `iperf` session it quickly reaches 1Gpbs rate. The attacker starts sending at t_1 at 1,000 pps (causing a minor glitch in the victim rate) and then injects the ACL in Fig. 6 at t_2, triggering thousands of MFC entries in the OVS data plane. In response, the victim rate rapidly drops by 80%. Then, at t_4, *the attacker increases its sending rate to* 2,000 *pps, resulting in a full denial of network service* to the victim. From that point, the victim rate drops close to 0 for 30 seconds, during which OVS can hardly push any useful packets through the data plane because of the malicious activity of the attacker. During our evaluations, we have seen similar cases of full-blown DoS under various scenarios, with cases when `iperf` could not even establish a new TCP session for extended periods of time.

6 GENERAL TSE

Next, we scrutinize the efficiency of the TSE attack when having co-located resources and knowledge about the ACLs are *not required*. Such alleviated requirements make *General TSE* attack more appealing as any arbitrary service, i.e., ACL, can be attacked. However, this comfort comes at a price that the attack itself requires more effort (in terms of packet rate) to even approximate the efficiency of *Co-located TSE* yet keeping the attack rate low ($\ll$ volumetric).

Correspondingly, in this section we first discuss how to generate a packet trace against an unknown ACL. Then, we show lower bounds on the estimated number of MFC masks we can achieve in all use cases against the ACL in Fig. 6), which we underpin later with practical measurements.

6.1 Adversarial Packet Trace

To target an unknown ACL, a naïve approach would generate sequentially all possible packets for the given header fields in order to spawn as many MFC masks as possible. Clearly, such approach would easily result in a volumetric attack since considering even the case of SipDp, the required successful attack rate would be $\sim$ 2.9 p(eta)bps. Therefore, we need a better heuristic algorithm that tries to approximate the attainable number of MFC masks. Randomization has proven to be efficient many times in practice (e.g., evolutionary and genetic algorithms, runtime analysis, convergence [9]), thus we adapt this approach to our packet trace generation. First, we analyse what are the chances that a packet with random (but legitimate) header will spawn an MFC entry. Then, we show what is the expected number of MFC masks for a given number of random packets sent to an unknown ACL.

Single Header. One can see in Fig. 3 that for a header length h the probability that one packet will spawn a specific entry in the MFC is $p_k(MFC) = \frac{2^k}{2^h}$, where k is the number of wildcarded bits the given MFC entry has; e.g., #2 entry in Fig. 3 $p_2(MFC) = \frac{2^2}{2^3} = 0.5$. Generally, the probability that from n randomly generated packets there will be *at least 1* packet that sparks an MFC entry for a given k is:

$$p_{(k,n)}(MFC) = 1 - (1 - p_k(MFC))^n. \quad (1)$$

Accordingly, the expected value of the number of MFC masks can be formalized as follows:

$$\mathbb{E}_{(k,n)}(MFC) = \sum_{k=0}^{h} C_k * p_{(k,n)}(MFC), \quad (2)$$

where C_k notes the number of different MFC entries for a given k.

Multiple Headers. Eq. 1 and Eq. 2 can be generalized to multiple headers; one only needs to pay attention to the number of possible different MFC mask combinations (C_k) for a given k, which heavily depends on the width of the header the first flow rule matches on (see Appendix for more details).

Note that for each use case all related header fields were randomized (e.g., for SipDp the packet trace contained packets with random source IP and destination port). Similarly to *Co-located TSE*, the traces included additional random noise to exhaust the *microflow cache*. Recall, it is usually used up in normal operation.

6.2 Synthetic Tests

Next, we show to what extent a practical random packet trace generation is in par with the expected values above.

Note that in our evaluation we used the same ACLs as well as the same testbed presented in §5, however, the attacker targets the ACL installed by the victim (ACL-V). For brevity, we only present the results for the synthetic tests, but note that as long as the *General TSE* attack achieves the same amount of MFC masks as *Co-located TSE*, the effects are the same irrespectively to the environment.

Results are depicted in Fig. 9b, where on the x axis the number of different random packets is shown, while the y axis depicts the expected (E) and measured (M) (averaged over 100 runs) MFC masks for each use case. Since the expected values are dominated by the width of the header the first flow rule of the ACL matches on (cf. §6.1), the difference between SipDp and SpDp was negligible; hence the latter is removed for brevity.

Observe that the more different header fields the ACL consists of the more MFC entries can be spawned with the same number of random packets. In particular, the maximum attainable MFC masks (with 50,000 packets) are approx. 16, 121, 122, and 581 in case of Dp, SpDp, SipDp, and SipSpDp, respectively. In terms of service degradation, these results mean that *General TSE* can reduce the full capacity with GRO OFF to 52% (97% with GRO ON, 88% with FHO, 60% with UDP), 12% (96% with GRO ON, 87% with FHO, 15.8% with UDP), and 1% (73.5% with GRO ON, 25.5% with FHO, 3.25% with UDP), respectively.

Recall that in *Co-located TSE* the maximum attainable MFC masks (17 for Dp, 256 for SpDp, 512 for SipDp, and 8195 for SipSpDp, respectively) require the same amount of packets. This means that for the Dp use case, *General TSE* can be as good as *Co-located TSE* in terms of attainable MFC masks. As *Co-located TSE* requires roughly 1,000 packets (0.67*Mbps*) do tear down OVS in the most complex use case, it can be seen that the same amount of random packets in case of *General TSE* is sufficient to degrade the useful capacity to 72.8% with GRO OFF (99.15% with GRO ON, 91.25% with FHO, 77.28% with UDP), 25.4% with GRO OFF (96.8% with GRO ON, 87.95% with FHO, 32.35% with UDP), and 11.7% with GRO OFF (95.8% with GRO ON, 87% with FHO, 12.5% with UDP) for Dp, SpDp/SipDp, and SipSpDp, respectively.

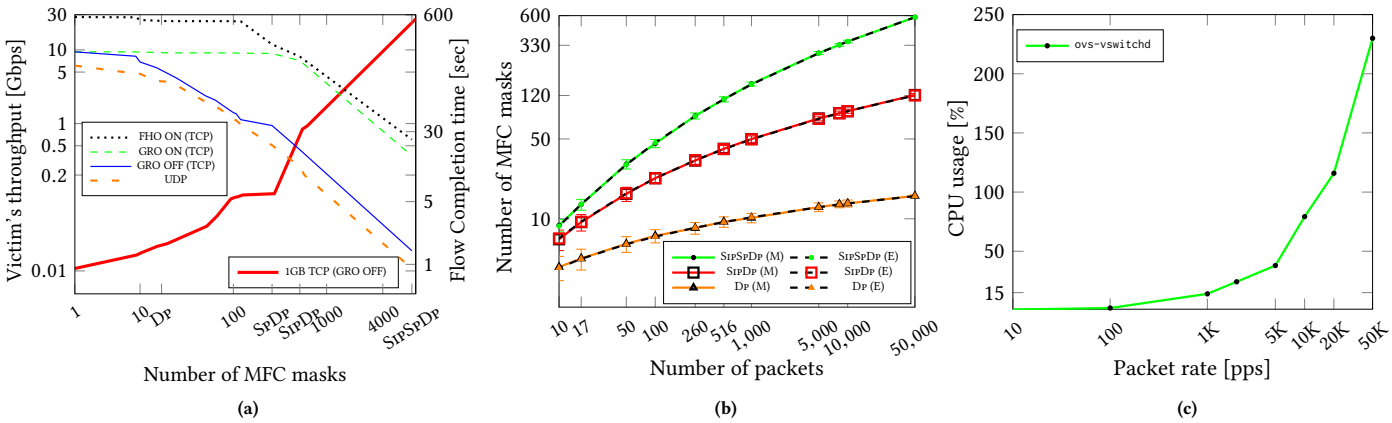

Figure 9: UDP and TCP (with GRO ON/OFF and FHO ON) throughput and flow completition time on the secondary y axis of the victim's traffic as the number of MFC masks increases (a); Average number of the expected (E) and measured (M) MFC masks attainable with *General TSE* (b); CPU usage of `MFCGuard` (axis x is in log scale) (c)

7 DISCUSSION

The technique extends to an arbitrary number of protocol fields. Each CMS imposes its own set of limitations on the possible ACLs that can be installed and the extent to which different packet header fields can be considered: by default, OpenStack and Kubernetes allow *ingress* policies to filter only on the source IP addresses and the destination port (TCP or UDP) [15, 70]. This gives a comfortable 32∗16 = 512 excess masks in the MFC. Calico (a Kubernetes network plugin [65]) allows ingress security policies to also filter on the source port, yielding possibly 8192 masks (already enough for a full-blown DoS) to which *egress* policies introduce the destination IP address as well (~ 200 thousand masks).

All cloud deployments implementing ACLs in OVS are affected. OVS is extensively used in cloud-based systems (e.g., it is the most widely used hypervisor switch in OpenStack) and it increasingly takes over the responsibility of enforcing ACLs from `iptables` due to the raw performance edge, standard support, and ease in management [56]. The TSE attack is effective over the OVN backend for OpenStack Neutron [72], OpenStack/OpenDaylight [69], OpenStack/ONOS [67], and in Kubernetes/OVN as demonstrated in §5.5 and §5.6. Note, however, that default installations are not directly affected as ACLs are implemented in `iptables`, but this architecture tends to become legacy soon [4]. Furthermore, major cloud providers do not seem to be affected: for instance, Microsoft Azure does not use OVS in the AccelNet network virtualization framework [28] and, even though the Google Cloud Platform *does* include OVS in the Andromeda data plane, this seems to be a significantly stripped down version [21]. In any case, we did not perform specific tests in public cloud providers' DCs for obvious ethical reasons.

TSE generalizes beyond OVS. TSE exploits an algorithmic complexity deficiency in the venerable TSS scheme. Therefore, deployments relying on the TSS scheme for packet classification, e.g., OpenStack/Networking-vpp [71], Contiv/VPP Kubernetes [25], Xen/HyperSwitch [59], Netronome SmartNIC [49], might be also affected; the evaluation has bee left for a future study.

Furthermore, there is considerable base of network-function virtualization [33, 48], cloud gateway/load-balancer [48], campus and enterprise networks [47] that use TSS scheme for packet classifier to implement non-trivial packet processing pipelines. If any of the flow tables in these deployments contain the above adversarial pattern, then the DoS attacks presented here are effective.

8 MITIGATION

The above results suggest that TSE can be particularly damaging. Accordingly, we initiated a responsible disclosure process by providing code and methodology to reproduce the synthetic tests to the corresponding security teams [11, 17, 18]. Besides, several immediate yet impractical remedies might help: *(i)* deploying or offloading ACL implementations to a different hypervisor switch (e.g., [34, 48, 78]) or to the *(ii)* high-performing gateway appliance (e.g., [6]), *(iii)* switching the MFC completely off, or *(iv)* enabling advanced flow caching via DPDK-based OVS datapath [23]. However, each of the above has the following corresponding disadvantage: in case of *(i)* other implementations might suffer from the same attack (e.g., [25, 26, 74]) or *(ii)* they do not help against attacks initiated within the DC, for *(iii)* MFC has been the biggest performance improvement so far [55], and for *(iv)* the feature that *may* prevent the attack is available in select datapaths.

Forcing the use of *jumbo frames* and *TCP buffers* (cf. §5.4) can substantially decrease the effective packet rate, however packets coming from outside might be limited to the default MTU size. And they do not cover attack against other traffic; e.g., UDP, which is the underlying transport protocol in QUIC [66].

`MFCGuard`. As a more customized mitigation technique we developed `MFCGuard`, which monitors and modifies the MFC—if the number of masks exceed a certain threshold, it looks for patterns corresponding to a possible TSE attack (cf. §3) in every 10 seconds, and wipes out those entries accordingly. We observed that monitoring (and modifying) the MFC has no overhead on the performance. In essence, removing an entry from the MFC means that matching packets will be processed in the slow path again. Since the slow path would spark the same MFC entries again, the idea behind `MFCGuard` was to constantly keep those entries out of the fast path. In practice, however, we observed that once an MFC entry is deleted then it will never be sparked again, i.e., matching packets will always be processed by the slow path. Such undesired, unexpected

and undocumented behavior [12] can have serious performance penalties; although MFC entries can be manually re-injected.

There are several requirements `MFCGuard` needs to meet: *(i)* entries covering the useful traffic should never be deleted. Furthermore, *(ii)* according to the available resources, we can only remove select flows from the MFC to find a balance between the maximum performance of the fast path and the increased resource utilization by the slow path; both impacting the overall quality of the run services. Due to requirement *(i)* `MFCGuard` will only remove entries with `drop` action! With this simple yet important requirement, *only* adversarial packets will be subjected to the slow path, keeping the fast path accelerated for the useful traffic flows (cf. Alg. 2 in §11.4). In our current implementation, we have therefore focused on *(i)*, leaving *(ii)* for future work.

We evaluated the efficiency of `MFCGuard` in all use cases (by deleting all drop rules) and observed that once the MFC is "cleaned", the performance of the victim's traffic goes back to its baseline. As the slow path is becoming much more involved, we evaluated the system's load in such cases. Results are depicted in Fig. 9c, where x and y axes show the attack rate and the corresponding CPU usage of the slow path daemon (`ovs-vswitchd`), respectively.

It can be seen that as long as the attack rate is less than 1, 000 pps ($<$ 1 Mbps) the slow path only consumes 15% of the CPU; recall, this packet rate is enough to bring down OVS in case of *Co-located TSE*). However, when the packet rate is 10, 000 pps, the CPU load jumps up to $\approx$ 80% (this rate in case of *General TSE* would be enough to degrade the full capacity to 10%). We can conclude that our current `MFCGuard` implementation is already capable of efficiently mitigating both TSE attacks as long as the attacking rate is low. If the attack rate is much above 10, 000 pps, the attack becomes a volumetric attack, for which there are multiple solutions to detect and handle (e.g., excess amount of packets and over-provisioning).

9 RELATED WORK

Whether or not to virtualize services is a complicated question many enterprises are facing today [24]; in a survey, 73% of responders said that security is a top challenge holding back cloud adoption [62], with the possibility of *unmediated* sharing and communications between different tenants' workloads being among the major concerns [53]. Such unmediated tenant-to-tenant interaction might be initiated by a malicious user by first launching a co-residency attack in order to co-locate a virtual machine with the target tenants' virtual machines on the same physical server [75], and then exploiting a side-channel effect [40, 44] to eavesdrop on sensitive information [22, 60].

Direct attacks on the cloud network infrastructure are less known; there has been work on fuzzing the data plane with considerable success [51, 73] and compromising SDN controllers [7]. Denial of service using algorithmic complexity attacks [2, 14, 16, 54] on the network data plane usually works by exploiting a vulnerable algorithm/data structure that is *already* in the targeted binary; e.g., [77] shows cache-collision attacks against the Linux IP stack and [20] targets *stateful* firewalls. Here, we showed a vulnerable data structure in the TSS scheme heavily used for packet classification in hypervisor switches. We showed that a typical ACL can be the vulnerable target itself in the data plane. Our finding can be exploited either remotely from the public Internet, or leasing a single virtual machine deployed in the cloud; detection and prevention techniques for algorithmic complexity attacks (see e.g., [5, 38, 54]) do not seem effective against it. Although, a mitigation technique for an algorithmic complexity attack in DPI engines [3] uses similar approach as our `MFCGuard`: a devised algorithm is used, which has a constant (but less than normal) throughput regardless of the input. The authors' aim is to dynamically shift between algorithms for normal and malicious input. In contrast, `MFCGuard` does not need to change algorithms at all, and always provides the highest attainable throughput regardless of the low-rate input.

10 CONCLUSION

Highly efficient and resilient packet classification is crucial to many security primitives particularly in a virtualized environments. In this paper, we investigate to what extent the TSS algorithm used in many software switches is vulnerable against low-rate DoS attacks. Our TSE attack exploits the fundamental space/time complexity of the TSS algorithm, and degrades the switch performance to 12% with low attack rate (0.7 Mbps). We show that if an adversary has knowledge of the used classification policies, she can virtually bring down the packet classifier with the same attack rate. One key aspect of our TSE attack is that it is hard to detect the attack as it does not uses any specific traffic pattern but some random packets. Furthermore, since we exploit a vital complexity characteristic, there seems to be no complete mitigation technique, unfortunately. As a short-term solution, we propose `MFCGuard`, a monitoring system that via carefully managing the entries in the tuple space can keep packet classification fast.

ACKNOWLEDGEMENTS

This research is supported by the National Research Foundation, Prime Minister's Office, Singapore under its Corporate Laboratory@University Scheme, National University of Singapore, and Singapore Telecommunications Ltd.

This research has also been supported by European Cooperation in Science and Technology (COST) Action CA 15127: RECODIS – Resilient communication and service, the UK Engineering and Physical Sciences Research Council (EPSRC) projects EP/N033957/1, and EP/P004024/1.

G. Rétvári has been supported by project no. 123957, 129589 and 124171 with the support provided from the National Research, Development and Innovation Fund of Hungary under the FK-17, KH-18 and K-17 funding schemes.

REFERENCES

[1] A Linux Foundation Collaborative Project. Production Quality, Multilayer Open Virtual Switch. http://www.openvswitch.org/, Accessed: June 2019.

[2] Afek, Y., Bremler-Barr, A., Harchol, Y., Hay, D., and Koral, Y. Making DPI engines resilient to algorithmic complexity attacks. *IEEE/ACM Transactions on Networking 24*, 6 (2016), 3262–3275.

[3] Afek, Y., Bremler-Barr, A., Harchol, Y., Hay, D., and Koral, Y. Making dpi engines resilient to algorithmic complexity attacks. *IEEE/ACM Transactions on Networking 24*, 6 (December 2016), 3262–3275.

[4] Ajo, M., Graf, T., Lazzaro, I., and Pettit, J. Taking security groups to ludicrous speed with OVS. In *OpenStack Summit* (2015).

[5] Alam, M. J., Goodrich, M. T., and Johnson, T. J-Viz: Finding algorithmic complexity attacks via graph visualization of Java bytecode. In *IEEE Symposium on Visualization for Cyber Security* (2016), pp. 1–8.

[6] Amazon Web Services. Elastic Load Balancing features. https://aws.amazon.com/elasticloadbalancing/features/#Details_for_Elastic_Load_Balancing_Products, Accessed in Jun 2019.

[7] Antikainen, M., Aura, T., and Särelä, M. Spook in your network: Attacking an SDN with a compromised OpenFlow switch. In *NordSec* (2014), pp. 229–244.

[8] Arins, A. Firewall as a service in sdn openflow network. In *2015 IEEE 3rd Workshop on Advances in Information, Electronic and Electrical Engineering (AIEEE)* (Nov 2015), pp. 1–5.

[9] Auger, A., and Doerr, B. *Theory of Randomized Search Heuristics*. WORLD SCIENTIFIC, 2011.

[10] Baboescu, F., Singh, S., and Varghese, G. Packet classification for core routers: Is there an alternative to CAMs? In *Int. Conf. Comput. Commun.* (Apr 2003), pp. 53–63.

[11] Ben Pfaff. OVS Orbit podcast. https://ovsorbit.org/episode-67.mp3, 2018.

[12] Ben Pfaff. [ovs-discuss] ovs-dpctl del-flow works strange. Mailing list archive, https://mail.openvswitch.org/pipermail/ovs-discuss/2019-June/048887.html, 2019 June.

[13] Casado, M., Koponen, T., Moon, D., and Shenker, S. Rethinking packet forwarding hardware. In *HotNets* (2008).

[14] CheckMarx. Regular expression Denial of Service: ReDoS, 2017. https://www.owasp.org/index.php/Regular_expression_Denial_of_Service_-_ReDoS.

[15] Cloud Native Computing Foundation. Network Policies. https://kubernetes.io/docs/concepts/services-networking/network-policies.

[16] Crosby, S. A., and Wallach, D. S. Denial of service via algorithmic complexity attacks. In *USENIX Security* (2003), pp. 3–3.

[17] Csikor, L., and Rétvári, G. The discrepancy of the megaflow cache in ovs. In *Open vSwitch Fall Conference* (Club Auto Sport, Santa Clara, CA, 2018).

[18] Csikor, L., Rothenberg, C., Pezaros, D. P., Schmid, S., Toka, L., and Rétvári, G. Policy injection: A cloud dataplane dos attack. In *Proceedings of the ACM SIGCOMM 2018 Conference on Posters and Demos* (New York, NY, USA, 2018), SIGCOMM '18, ACM, pp. 147–149.

[19] Csikor, L., Szalay, M., Sonkoly, B., and Toka, L. NFPA: Network function performance analyzer. In *IEEE NFV-SDN, Demo Track* (2015), pp. 17–19.

[20] Czubak, A., and Szymanek, M. Algorithmic complexity vulnerability analysis of a stateful firewall. In *ISAT* (2017), pp. 77–97.

[21] Dalton, M., et al. Andromeda: Performance, isolation, and velocity at scale in cloud network virtualization. In *USENIX NSDI* (2018), pp. 373–387.

[22] Delimitrou, C., and Kozyrakis, C. Bolt: I know what you did last summer... in the cloud. In *ASPLOS* (2017), pp. 599–613.

[23] DPDK. Membership Library. https://doc.dpdk.org/guides/prog_guide/member_lib.html.

[24] et al., T. K. Network virtualization in multi-tenant datacenters. In *NSDI* (2014), pp. 203–216.

[25] FD.io. Contiv/VPP Kubernetes Network Plugin. https://fdio-vpp.readthedocs.io/en/latest/usecases/contiv/K8s_Overview.html.

[26] FD.io. VPP - Vector Packet Processing. https://docs.fd.io/vpp/19.01/index.html.

[27] Feldman, A., and Muthukrishnan, S. Tradeoffs for packet classification. In *INFOCOM* (2000), vol. 3, pp. 1193–1202.

[28] Firestone, D., et al. Azure accelerated networking: SmartNICs in the public cloud. In *USENIX NSDI* (2018), pp. 51–66.

[29] Gobriel, S., and Tai, C. OvS Lookup Optimization Using Two-Layer Table Lookup. In *Open vSwitch Fall Conference* (2016).

[30] Gupta, P., and McKeown, N. Packet classification on multiple fields. In *SIGCOMM* (1999), pp. 147–160.

[31] Gupta, P., and McKeown, N. Algorithms for packet classification. *IEEE Network 15*, 2 (2001), 24–32.

[32] Gupta, P., and McKeown, N. Algorithms for packet classification. *Netwrk. Mag. of Global Internetwkg. 15*, 2 (2001), 24–32.

[33] Intel. Network function virtualization: Quality of Service in Broadband Remote Access Servers with Linux and Intel architecture. https://networkbuilders.intel.com/docs/Network_Builders_RA_NFV_QoS_Aug2014.pdf.

[34] ioVisor. eXpress Data Path, 2016. https://www.iovisor.org/technology/xdp.

[35] Istio. Authentication Policy, 2018. https://istio.io/docs/reference/config/istio.authentication.v1alpha1.

[36] Istio. Ingress Controller, 2018. https://istio.io/docs/tasks/traffic-management/ingress.html.

[37] Istio. Traffic Routing, 2018. https://istio.io/docs/reference/config/istio.networking.v1alpha3.

[38] Khan, S., and Traore, I. A prevention model for algorithmic complexity attacks. In *DIMVA* (2005), pp. 160–173.

[39] Kim, C., Caesar, M., Gerber, A., and Rexford, J. Revisiting route caching: The world should be flat. In *PAM* (2009), pp. 3–12.

[40] Kocher, P., Genkin, D., Gruss, D., Haas, W., Hamburg, M., Lipp, M., Mangard, S., Prescher, T., Schwarz, M., and Yarom, Y. Spectre Attacks: Exploiting Speculative Execution. *ArXiv e-prints* (Jan. 2018).

[41] Kogan, K., et al. SAX-PAC: scalable and expressive packet classification. In *SIGCOMM* (2014), pp. 15–26.

[42] Kuzmanovic, A., and Knightly, E. W. Low-rate tcp-targeted denial of service attacks: the shrew vs. the mice and elephants. In *Proceedings of the 2003 conference on Applications, technologies, architectures, and protocols for computer communications* (2003), ACM, pp. 75–86.

[43] Lim, H., Lee, N., and Lee, J. Multi-match packet classification scheme combining tcam with an algorithmic approach. *IEIE Transactions on Smart Processing and Computing 6*, 1 (Febr 2017), 27–38.

[44] Lipp, M., Schwarz, M., Gruss, D., Prescher, T., Haas, W., Mangard, S., Kocher, P., Genkin, D., Yarom, Y., and Hamburg, M. Meltdown. *ArXiv e-prints* (Jan. 2018).

[45] Liu, X., Cho, B., and Kim, J. Sd-ovs: Syn flooding attack defending open vswitch for sdn. In *WISA* (03 2017), pp. 29–41.

[46] Liu, Y., Amin, S. O., and Wang, L. Efficient FIB caching using minimal non-overlapping prefixes. *SIGCOMM Comput. Commun. Rev. 43*, 1 (2013), 14–21.

[47] McKeown, N., Anderson, T., Balakrishnan, H., Parulkar, G., Peterson, L., Rexford, J., Shenker, S., and Turner, J. OpenFlow: enabling innovation in campus networks. *SIGCOMM Computer Communication Review 38*, 2 (2008), 69–74.

[48] Molnár, L., Pongrácz, G., Enyedi, G., Kis, Z. L., Csikor, L., Juhász, F., Kőrösi, A., and Rétvári, G. Dataplane specialization for high-performance OpenFlow software switching. In *SIGCOMM* (2016), pp. 539–552.

[49] Netronome. Agilio OVS Software Architecture for Server-based Networking. Whitepaper, 2018. https://www.netronome.com/media/documents/WP_Agilio_SW.pdf.

[50] Newman, P., Minshall, G., and Lyon, T. L. IP switching – ATM under IP. *IEEE/ACM Trans. Netw. 6*, 2 (1998), 117–129.

[51] Nicholas Gray, Manuel Sommer, T. Z., and Tran-Gia, P. FlowFuzz: a framework for fuzzing openflow-enabled software and hardware switches. In *Black Hat* (2017).

[52] The Open Networking Foundation. *OpenFlow Switch Specifications v.1.4.0*, 2013.

[53] Pearce, M., Zeadally, S., and Hunt, R. Virtualization: Issues, security threats, and solutions. *ACM Comput. Surv. 45*, 2 (2013), 17:1–17:39.

[54] Petsios, T., Zhao, J., Keromytis, A. D., and Jana, S. SlowFuzz: Automated domain-independent detection of algorithmic complexity vulnerabilities. In *ACM CCS* (2017), pp. 2155–2168.

[55] Pettit, J. Accelerating Open vSwitch to "Ludicrous Speed. Blog post: Network Heresy - Talses of the network reformation, 2014. https://networkheresy.com/2014/11/13/accelerating-open-vswitch-to-ludicrous-speed/.

[56] Pfaff, B., and Davie, B. The Open vSwitch database management protocol. RFC 7047, 2013.

[57] Pfaff, B., Pettit, J., Koponen, T., Jackson, E., Zhou, A., Rajahalme, J., Gross, J., Wang, A., Stringer, J., Shelar, P., Amidon, K., and Casado, M. The design and implementation of Open vSwitch. In *NSDI* (2015), pp. 117–130.

[58] Pong, F., and Tzeng, N.-F. Hashing round-down prefixes for rapid packet classification. In *USENIX Annual Technical Conference* (2009).

[59] Ram, K. K., Cox, A. L., Chadha, M., and Rixner, S. Hyper-Switch: A Scalable Software Virtual Switching Architecture. In *Usenix ATC* (2013), p. 12.

[60] Ristenpart, T., Tromer, E., Shacham, H., and Savage, S. Hey, you, get off of my cloud: Exploring information leakage in third-party compute clouds. In *ACM CCS* (2009), pp. 199–212.

[61] Schuchard, M., Thompson, C., Hopper, N., and Kim, Y. Taking routers off their meds: Unstable routers and the buggy bgp implementations that cause them. Tech. rep., tech. rep., University of Minnesota, 2011.

[62] SecurityWeek. CSA's cloud adoption, practices and priorities survey report, 2015. http://www.securityweek.com/data-security-concerns-still-challenge.

[63] Shelly, N., Jackson, E. J., Koponen, T., McKeown, N., and Rajahalme, J. Flow caching for high entropy packet fields. *SIGCOMM Comput. Commun. Rev. 44*, 4 (2014).

[64] Srinivasan, V., Suri, S., and Varghese, G. Packet classification using tuple space search. In *SIGCOMM* (1999), pp. 135–146.

[65] The Calico project. https://www.projectcalico.org/.

[66] The Chromium Projects. QUIC, a multiplexed stream transport over UDP. https://www.chromium.org/quic, 2019.

[67] The ONOS project. Security Group. https://wiki.onosproject.org/display/ONOS/Security+Group.
[68] The Open vSwitch project. Kubernetes integration for OVN. https://github.com/openvswitch/ovn-kubernetes.
[69] The OpenDaylight project. OVSDB:Security Groups. https://wiki.opendaylight.org/view/OVSDB:Security_Groups.
[70] The OpenStack project. Manage project security. https://docs.openstack.org/nova/pike/admin/security-groups.html.
[71] The OpenStack project. Networking-vpp. https://wiki.openstack.org/wiki/Networking-vpp.
[72] The OpenStack project. OpenStack Neutron integration with OVN. https://docs.openstack.org/networking-ovn/latest.
[73] Thimmaraju, K., Shastry, B., Fiebig, T., Hetzelt, F., Seifert, J., Feldmann, A., and Schmid, S. Taking control of sdn-based cloud systems via the data plane. In *ACM Symposium on SDN Research (SOSR)* (2018).
[74] Tollet, J. Networking-VPP: A fast forwarding vSwitch/vRouter for OpenStack. In *FOSDEM* (2018).
[75] Varadarajan, V., Zhang, Y., Ristenpart, T., and Swift, M. A placement vulnerability study in multi-tenant public clouds. In *USENIX Security* (2015), pp. 913–928.
[76] Varvello, M., Laufer, R., Zhang, F., and Lakshman, T. Multi-Layer Packet Classification with Graphics Processing Units. In *Proceedings of the 10th ACM International on Conference on emerging Networking Experiments and Technologies - CoNEXT '14* (Sydney, Australia, 2014), ACM Press, pp. 109–120.
[77] Weimer, F. Algorithmic complexity attacks and the linux networking code, 2003. http://www.enyo.de/fw/security/notes/linux-dst-cache-dos.html.
[78] Zhou, D., Fan, B., Lim, H., Kaminsky, M., and Andersen, D. G. Scalable, high performance Ethernet forwarding with CuckooSwitch. In *CoNEXT* (2013), pp. 97–108.

11 APPENDIX

11.1 OVS cache infrastructure

The OVS flow cache infrastructure and the whole pipeline of processing a packet through the caches all the way up to the slow path (in case of the first packet of the flow) is shown in Fig. 10.

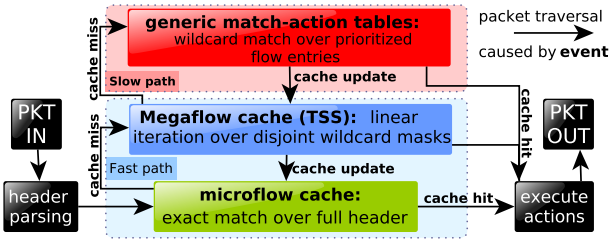

Figure 10: The OVS flow cache infrastructure.

11.2 Megaflow Lookup Algorithm

With the invariants (Inv(1)) and (Inv(2)) described in §3.2 is mind we summarize a rather simplified description of the MFC lookup algorithm implemented in the OVS fast path below:

Algorithm 1 Megaflow lookup. *Input:* packet header h

for $M \in \mathcal{M}$ **do**
  lookup (h *AND* M) in the hash H_M
  if found *then return* cache hit
end for
return cache miss

Proof of Theorem 4.1. Let parameter $k = |\mathcal{M}|$ denote the number of masks and let B_i be the set of bitpositions used by the i-th mask. It is easy to see that the number of keys in the MFC is minimal if $B_i \cap B_j = \emptyset$ for $1 \leq i < j \leq k$. In this case, to cover each denied packet the i-th mask needs $2^{b_i} - 1$ keys (each key except the one that refers to the allow rule), where b_i is the number of bit positions set in B_i. Thus, the number of keys in the MFC is $\sum_i \left(2^{k_i} - 1\right)$. Using the inequality between geometric and arithmetic means, the expression $\sum_i 2^{b_i}$ subject to $\sum_i b_i = w$ takes the minimal value when $k2^{\frac{w}{k}}$. Hence, for k masks the number of keys is at least $k2^{\frac{w}{k}} - k = O(k2^{\frac{w}{k}})$. □

Proof of Theorem 4.2. We focus only on the keys that refer to `deny` packets. Since there is an `allow` rule for each field, all masks must refer to every field on at least one position. One can see that to minimize the number of keys these positions should be a Cartesian product of separate solutions for the different fields. Let k_i be the number of masks considering only the i-th field, then using the result of Theorem 4.1 we get the required result. □

11.3 Probabilities and expected values

Multiple header fields with ACL unknown. Naïvely, one might think that for each k there is one combination where one of the headers has $k - l$ wildcarded bits, while the other header has l ($0 \leq l \leq k$). However, as can be seen in Fig. 5 according to the order of the flow rules in the flow table (cf. Fig. 4), only the first allow rule appears in the MFC cache in the same way, i.e., with the other header fully wildcarded. If the second flow rule was also represented in the same way, then the MFC would violate the *order-independent property* as a packet with *HYP* `001` and *HYP2* `1111` header would match on both of the entries. Therefore, for $k = l$ or $k = 0$ there is just one combination.

Furthermore, if k is greater than the length of the shortest header (s), then again the number of possible combinations is less (i.e., it simply cannot hold more wildcarded bits as its length s). These observations can be summarized as follows: for two different header fields of length s, l ($s \leq l$) : $C_k = k + 2$ if $0 \leq k < s$, $C_k = s$ if $s \leq k < l$, and $C_k = (s + l) - (k + 1)$ if $l \leq k$.

Thus, the most important factor in calculating of the expected values is C_k. In the following, how its calculation can be generalized to above 2 headers.

Assume that we have $m + 1$ different flow rules, where m rules match on m different headers with sizes of $h_1, h_2, \ldots, h_m$, where h_1 is the highest priority rule, while h_m is the lowest one. Additionally, the last rule ($(m + 1)^{th}$) is the low priority deny rule. The entries covering the $i{-}1^{th}$ rule contain prefix rules for the previous headers, exact match for the i^{th} header, and wildcard for the remaining headers. Let $f_{i-1}(u)$ be the number of combinations for prefix fields with u wildcarded bit. Then, it can be calculated by the following convolution:

$$f_i(k) = \sum_{j=1}^{\min(k,h_j)} f_{i-1}(k - j),$$

where $f_0(k) = 1_{k=0}$. Let f_m be the same for the deny rule, and it can calculated with the same convolution. Furthermore, let $C_k^{(i-1)}$ be the number of combinations that contain k wildcarded bits in the whole header, then it can be calculated as $C_k^{(i-1)} = f_{i-1}(k - \sum_{j=i+1}^{m} h_j)$. Therefore, $C_k = \sum_{i=0}^{m} C_k^{(i)}$.

11.4 Mitigation Algorithm

Below, we present the mitigation algorithm. First, it has two preset thresholds (for the number of MFC masks (m_th) as well as for the acceptable CPU overhead (c_th)) as input parameters that can be fine-tuned according to the available resources. As indicated in *Line 1*, the algorithm runs every 10 seconds according to the MFC eviction policy. In *Line 2*, we check the number of masks in the MFC (it can be acquired via commands `ovs-dpctl dump-flows` or `ovs-dpctl show`). If the number of MFC masks is above the preset threshold (*Line 3*), then for each rule in the FlowTable we look for a pattern the TSE attack would generate (according to §4) in the MFC (*Line 4*). If a pattern is found (*Line 6*), we remove the corresponding entries from the MFC (*Line 7*). Each time after removing some selected entries from the MFC, we check the increased CPU utilization (e.g., via command *top* in *Line 9*) and if it is below the threshold (*Line 10*), we keep removing MFC entries (if there are any); otherwise the system is considered to be balanced, i.e., no more entries from the MFC will be removed as it would cause too much packet processing overhead in the slow path.

Algorithm 2 Mitigation. *Input:* #MFC mask threshold `m_th`, CPU utilization threshold `c_th`

```
1:  for every 10 second do
2:      m ← checkNumberOfMasks()
3:      if m > m_th then
4:          for rule in FlowTable do
5:              found ← lookPatternInMFC(rule)
6:              if found then
7:                  deleteMFCEntries(rule)
8:              end if
9:              cpu_util ← checkCPUUtilization()
10:             if cpu_util ≥ c_th then
11:                 return
12:             end if
13:         end for
14:     end if
15: end for
```